High-pressure x-ray absorption study of GaTe including polarization

J. Pellicer-Porres,* A. Segura, and V. Muñoz
Institut de Ciència dels Materials, Universitat de València, Doctor Moliner 50, Edifici Investigació, E-46100 Burjassot, València, Spain

A. San Miguel
Département de Physique des Matériaux, Bâtiment 203, Université Lyon I, 43 Boulevard du 11 Novembre 1918, F-69622, Villeurbanne, France

(Received 7 June 1999; revised manuscript received 31 August 1999)

The evolution of the local structure in GaTe under pressure is studied by x-ray absorption spectroscopy experiments at the Ga *K*-edge (10.368 keV) on oriented single crystals. Taking advantage of the linearly polarized character of synchrotron radiation, the pressure evolution of both the Ga-Te and the in-plane Ga-Ga bond lengths could be determined, in spite of the small amplitude of the latter. Our measurements show that both distances are much less compressible than what could be inferred from the bulk compressibility, which evidences a strong variation of Ga-Ga-Te and Te-Ga-Te angles under pressure. The Te-Te intralayer distance perpendicular to the layers is observed to increase with increasing pressure. In the high-pressure NaCl phase, no anisotropy of the x-ray absorption fine structure spectrum is detected and local and bulk compressibilities coincide. With the help of microphotographic measurements the main source of instability of the layer structure is attributed to the tilt of the Ga-Ga bond with respect to the layer plane.

I. INTRODUCTION

Semiconductors from the III-VI layered family present strongly anisotropic physical properties, whose description demands for theoretical models that could be able to simultaneously describe electronic interactions of very different nature. Under high pressure, the strength of intra- and interlayer interactions evolve in a drastically different manner, and the evolution of the associated physical properties constitute a strong test of validity of theoretical models. In this family of III-VI layered materials, the covalent layers are separated by the so-called van der Waals gap, with weak interactions of van der Waals type between the layers. Consequently, this gap follows a pressure evolution considerably different from the evolution of any characteristic distance inside the layers. Besides the fundamental interest of this type of materials, many technical applications have been proposed in the development of solar cells,[1–3] nonlinear optics,[4–9] or as candidates for solid-state batteries.[10–12]

GaTe is a member of the III-VI layered family (GaS, GaSe, GaTe, and InSe).[13] The monoclinic (B2/m) low-pressure modification[14] of GaTe [Fig. 1(a)] is a semiconductor with a band gap of 1.68 eV (Ref. 15) in ambient conditions. As in the other III-VI layered semiconductors,[16,17] bonds inside the layers are mainly covalent but, unlike GaS, GaSe, or InSe in which all cation-cation bonds are perpendicular to the layers, in GaTe one-third of the Ga-Ga bonds are parallel to the layers, giving rise to a supplementary cleaving plane along the *c* axis, so that the crystals can be very easily oriented. Figure 1(b) presents the top view of a single layer, where we have drawn the direction of the crystallographic *c* axis and its perpendicular in the layer plane for subsequent reference. The layers are bound mainly by van der Waals forces between Te atoms. The whole gives rise to quasitetrahedral coordination for the Ga atoms (three Te and one Ga) and threefold coordination for Te with Ga atoms. In average, the Hume-Rothery rule is preserved. We expect then a high anisotropy in bonding, which will manifest in the compressibilities, not only in the direction perpendicular to the layers plane, but also in the layer itself.

To our knowledge, GaTe has been studied under pressure by means of photoconductivity low-pressure experiments,[18] x-ray diffraction (XRD),[19] optical reflectivity,[19] and optical absorption.[20] By XRD experiments a first-order high-pressure transition to a high-pressure polymorph of the NaCl type was found at 10 ± 1 GPa. Optical reflectivity demonstrated the metallic character of the high-pressure phase. When decreasing pressure, the NaCl phase was observed down to 3.2 GPa, pressure at which the material became amorphous.[19] Photoconductivity experiments showed the shift of the direct band gap at low pressure. A more accurate and complete study of the direct band-gap evolution was carried out by optical-absorption measurements, where in addition it was extracted information about the indirect gap and the static dielectric constant.[20]

An essential problem in the description of the physical properties at high pressure in III-VI layered compounds is the lack of information concerning the pressure evolution of the atomic positions in the unit cell. To our knowledge it has only been possible in GaS.[21] This implies the introduction of additional assumptions in models to compute electronic band structure under pressure[22] and is a fundamental limitation for total-energy calculations. This problem can be attributed to experimental difficulties introduced by the layered character of the sample that on the one side makes it very difficult to obtain a pure single-crystalline sample (the presence of stacking defects or twinned planes is almost unavoidable) and on the other side introduces preferential orientation in powder samples. X-ray absorption spectroscopy[23] (XAS) is a very powerful technique that provides information on the pressure evolution of the local structure and is consequently an excellent complement for XRD studies at high pressure.[24] The combination of the two techniques has already been successful in the determination of the full structure of high-

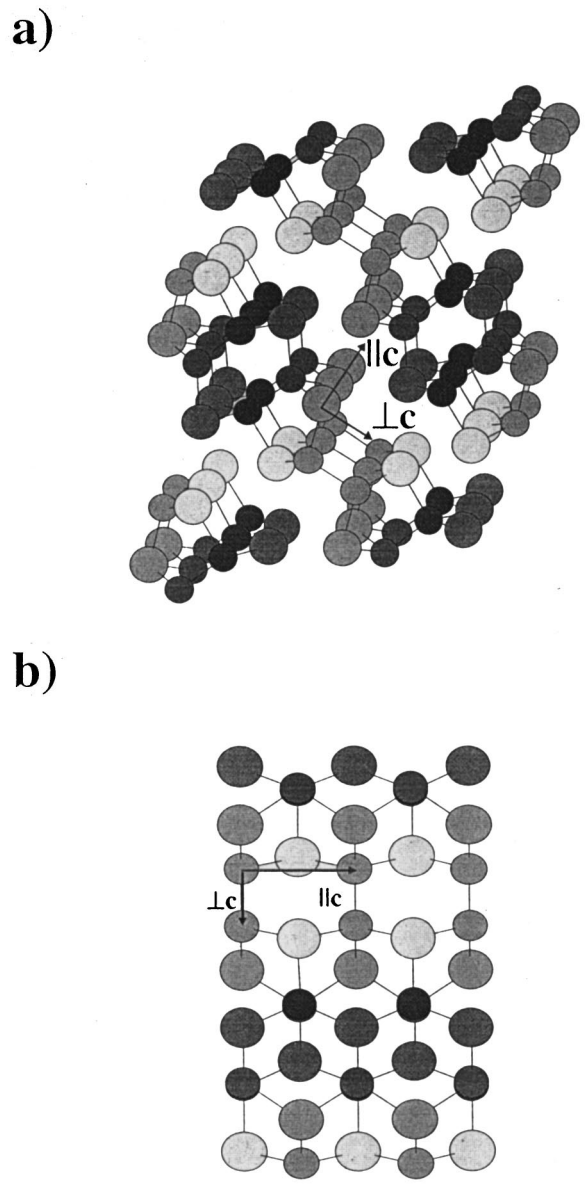

FIG. 1. (a) GaTe structure. (b) GaTe layer top view. In both drawings, the crystallographic *c* axis and its perpendicular (in the plane of the layer) are drawn. Nonequivalent atoms have different shadowing. Big and small circles correspond to Te and Ga atoms, respectively. View (b) corresponds to the plane of polarization of the x rays.

pressure structures of materials.[25,26]

Recently, XAS experiments under pressure have been carried out in single crystals of GaSe[27] and InSe.[26] The main conclusion obtained was the low compression of the cation-anion bond when compared with the variation of the *a* axis. The pressure variation of the bond length is only compatible with the variation of the lattice parameter *a* if one assumes a change in the cation-anion-cation and anion-cation-cation angles. Under plausible hypothesis, a description of the evolution of the full structure with pressure was given.[26]

In this paper we present an extended x-ray absorption fine structure (EXAFS) experiment in oriented GaTe single crystals at the Ga *K*-edge (10.368 keV) in order to study the evolution of the local structure under pressure. The synchrotron radiation polarization is used to separate the contribution from the Ga-Ga bonds that lie in the layer plane from the more intense Ga-Te contribution.

We also present the results of microphotographic measurements of the compressibility along the direction perpendicular to the *c* axis in the layer plane.

II. EXPERIMENT

High quality oriented GaTe needles were grown by vapor phase transport. The needles present natural faces parallel to the layers and natural edges parallel to the *c* axis. Samples were cut into parallelepipeds with typical dimensions of $100\times150\times30\ \mu m^3$. A wide angle aperture membrane diamond-anvil cell[28] (MDAC) was used as pressure generator. The diamonds were of the Drukker standard type, with culet size of 0.5 mm. The single-crystal sample was placed in a 250-μm diameter hole drilled in an Inconel gasket. Silicon oil was used as pressure transmitting medium, and the pressure was measured *in situ* using the linear ruby fluorescence scale.[29]

The XAS experiments were carried out at the ID24 energy dispersive x-ray absorption station of the European Synchrotron Radiation Facility (ESRF, Grenoble, France).[30] The undulator source provides linearly polarized photons in the horizontal plane. A profiled curved Si (111) monochromator[31] focused the beam to a spot of approximately 50 μm in the horizontal direction. In the vertical direction the beam was only slit to 100 μm. Details on the principle of energy dispersive x-ray absorption data collection can be found elsewhere.[32] An essential experimental aspect of XAS experiments at high pressure is the presence of glitches in the XAS spectra originated by XRD of the diamond single crystals. The pressure cell is oriented with respect to the polychromatic x-ray beam in order to remove these glitches from the widest spectral domain around the x-ray absorption edge. This operation takes advantage of the real time visualization of the XAS spectra thanks to the x-ray parallel collection characteristic of the energy dispersive setup. In addition, in our experiment, we needed to orient the sample with respect to the synchrotron radiation polarization vector to increase the signal coming from the Ga-Ga bond that lay in the layer plane with respect to the signal coming from the Ga-Te bond. Given the geometry of our experiment, the x-ray polarization vector is always in the layer plane. To give us the best chances of finding a good orientation of the cell plus sample system: (i) a wide angular aperture diamond-anvil cell was used. (ii) the sample was immobilized inside the cell by using a relatively viscous pressure transmitting media (silicon oil). For the first sample (sample A), we found two positions of the cell plus sample system where the polarization vector was parallel and perpendicular to the Ga-Ga bonds and where no diamond glitches appeared in the spectral domain of interest. For the second sample (sample B) we obtained two other orientations with the polarization vector forming angles of $\alpha=25°$ and $\alpha=65°$ with respect to the in-plane Ga-Ga bonds.

To determine the compressibilities of GaTe in the layer plane high-pressure microphotographic measurements were performed. A charge-coupled device (CCD) camera was inserted in the optical axis of a microscopic optical setup for absorption measurements in the MDAC (see, for instance,

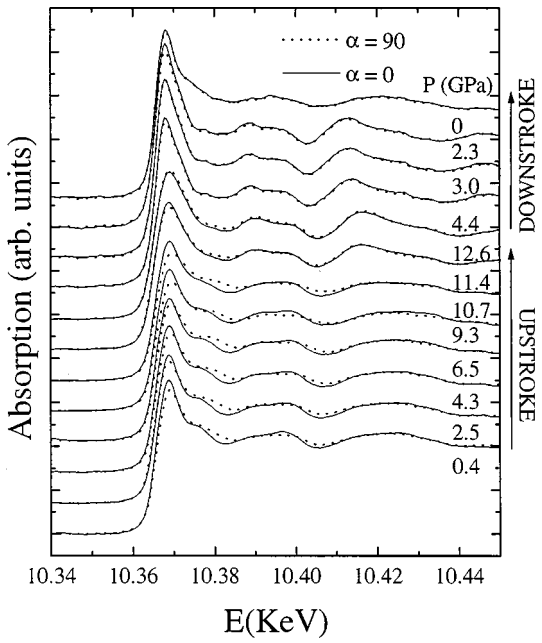

FIG. 2. GaTe XAFS spectra at several pressures. Dot lines: polarization vector in the plane of layers and perpendicular to the *c* axis (sample A, $\alpha=90$); continuous lines: polarization vector parallel to the *c* axis (sample A, $\alpha=0$).

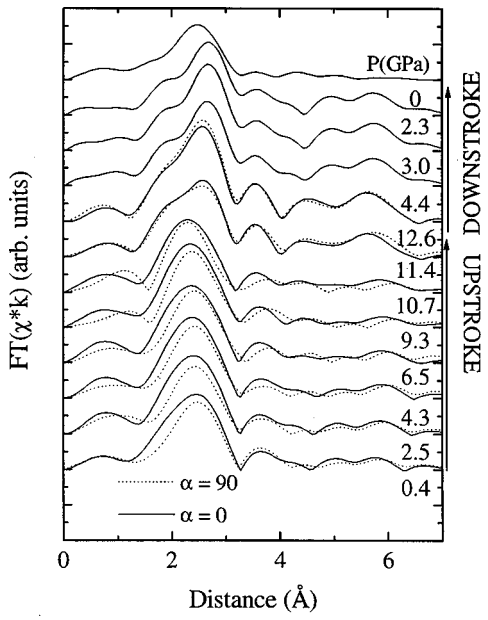

FIG. 3. Pair-pseudodistribution function (PPDF) obtained by Fourier transformation of the EXAFS signal. Dot lines: polarization vector in the plane of the layers and perpendicular to the *c* axis (sample A, $\alpha=90$); continuous lines: polarization vector parallel to the *c* axis (sample A, $\alpha=0$).

Refs. 33 and 34). In Ref. 34, Gauthier *et al.* verified that no systematic error is involved from a lens effect due to the deformation of the anvils up to 25 GPa. As we use the same type of MDAC and the maximum pressure was 20 GPa, we do not expect any lens effect. We employed the CCD images to measure the relative diminution in the length of the sample for different directions. The *c*-axis compressibility of GaTe (Ref. 19) was used as pressure gauge. The ruby fluorescence method was not used in order to avoid any source of error originated from the movement of the camera. The sample dimensions in the digital image were measured with a relative error of 2%.

III. RESULTS AND DISCUSSION

A. XANES

Normalized XANES (x-ray absorption near-edge structure) spectra for sample A are presented in Fig. 2 for several significant pressures. In the XANES regime, multiple scattering of the excited electrons confers sensitivity to the details of the spatial arrangement of atoms neighboring the absorbing one. The use of linearly polarized synchrotron radiation can bring to evidence the differences of local structure with respect to two spatial directions. In our experiment, x-ray linear dichroism is clearly observable in all the spectra from ambient pressure up to 10.7 GPa. From this spectrum on, XANES resonances start to change in both orientations of the sample and the x-ray linear dichroism disappears, coherently with the transition to the isotropic high-pressure NaCl structure described in XRD studies.[19] The high-pressure resonance pattern is maintained in the downstroke up to at least 2.3 GPa. Nevertheless, the recovered sample presents a net broadening of the structures and does not show any x-ray linear dichroism, suggesting the amorphous character of the sample after the pressure cycle.

We have used the XANES weighted average method[35] to deduce the proportion of local mixing spectra for pressures near the phase transition, and in this way determine the phase transition pressure. This study shows that the transition can be situated at 10.3 ± 1.0 GPa, in very good agreement with XRD experiments.[19]

B. EXAFS

1. Data analysis

The EXAFS (extended x-ray absorption fine structure) oscillations were extracted from the spectra coming from the two samples and for the two orientations of the cell. The presence of XRD glitches and some x-ray coherence effects limited the useful spectral range to 250 eV after the edge. The pair-pseudodistribution function (PPDF) is obtained by Fourier transformation of the EXAFS signal in a *k* domain between 2.36 and 7.90 Å and using a Bessel based apodization window ($\tau=2.5$). It is shown in Fig. 3 for different pressures (sample A). The peak extending from 1.2 to 3.2 Å corresponds to contributions coming from Te atoms at distances ranging from 2.637 to 2.686 Å. If the polarization vector has not the same direction as the *c* crystallographic axis ($\alpha\neq0$), the Ga-Ga bond parallel to the layers (2.436 Å) also contributes to the peak. The position and shape of this peak abruptly change for pressures higher than 10.7 GPa and maintains its structure in the downstroke up to at least 2.3 GPa. In the downstroke process we observed a progressive evolution of the PPDF, that strongly diminishes its amplitude and enlarges its width, indicating the appearance of structural disorder. As there is no linear dichroism, the isotropy of the structure is preserved in the process. The PPDF of the recovered sample is totally different from the PPDF of both the low- and high-pressure phases, and presents all characteristic

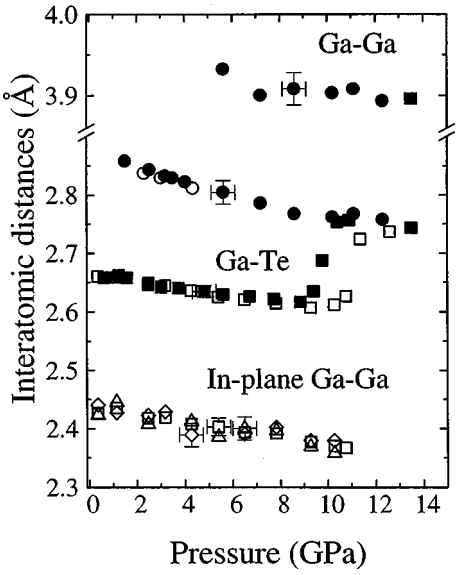

FIG. 4. Ga-Te and in-plane Ga-Ga distances obtained by a fit to the EXAFS part of the spectra. Squares: upstroke. Circles: downstroke. Hollow symbols: sample A. Filled symbols: sample B. Concerning the Ga-Ga data, the meaning of the symbols is: squares: phases and amplitudes for Ga-Te from the high-pressure modification, phases and amplitudes for Ga-Ga from the FEFF code. Triangles: phases and amplitudes for Ga-Te from the high-pressure modification, phases and amplitudes for Ga-Ga from the oriented-weighted difference between spectra with $\alpha=0°$ and $\alpha=90°$. Diamonds: phases and amplitudes for Ga-Te from the FEFF code, phases and amplitudes for Ga-Ga from the FEFF code.

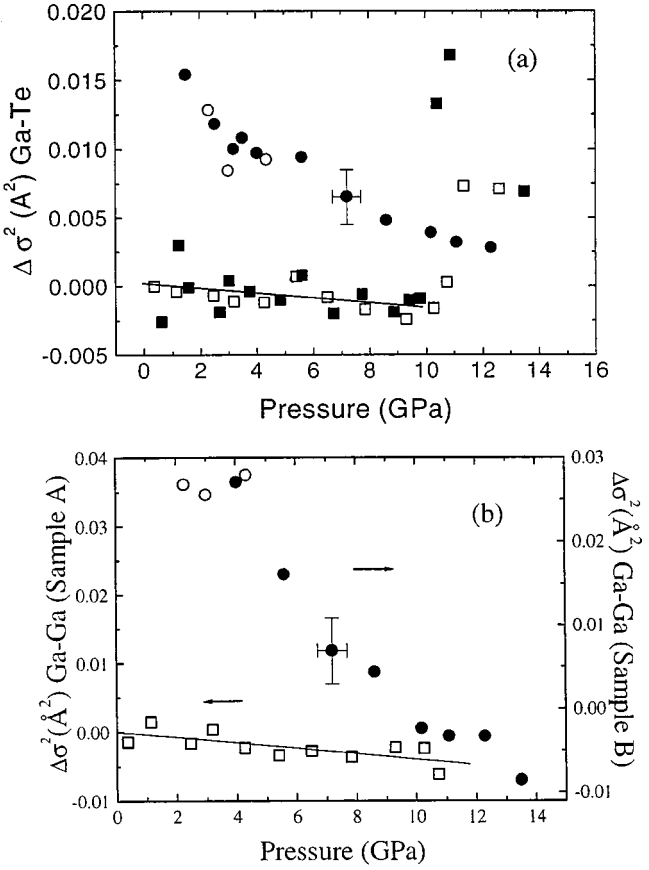

FIG. 5. EXAFS pseudo-Debye-Waller factor variation under pressure obtained in the EXAFS analysis for: (a) the Ga-Te bond, (b) the Ga-Ga bond. Squares: upstroke. Circles: downstroke. Hollow symbols: sample A. Filled symbols: sample B.

features of the spectrum of an amorphous sample, in well agreement with the findings of XANES in the previous section and those of XRD in Ref. 19.

The presence of multiple distances in the first neighbor shell prevents from using the ambient pressure spectra to directly extract the EXAFS phases and amplitudes that are needed in the analysis of higher pressure spectra. Instead, different methods were used for their calculation, all converging to give the same results. For $\alpha=0$ (sample A) and $\alpha=25$ (sample B) we extracted the phases and amplitudes corresponding to the Ga-Te backscattering process with two methods: (i) from the high-pressure spectra, where the structural data were known by XRD[19]—we employed only one distance in the fitting procedure, representing an average distance, and deduced pressure variations for the Ga-Te bond length (Fig. 4) and the corresponding increments in the EXAFS pseudo-Debye-Waller (DW) factor [Fig. 5(a)]; (ii) with phases and amplitudes from the FEFF code for *ab initio* calculation of multiple-scattering x-ray absorption fine structure.[36] In this case, phases and amplitudes were carefully studied to bunch them in three representative groups. Nevertheless, the high number of parameters involved in the fit compelled us to hold fixed the DW factors. With respect to the Ga-Te bond length variation, the deduced values presented the same overall behavior as in case (i), but were more dispersed. We consider more reliable the data obtained with method (i). In addition, no matter which method is employed, in the high-pressure phase it is possible to extend the analysis to the second shell of neighbors.

For $\alpha=90$ (sample A), the average Ga-Te bond length previously extracted from the spectra taken with $\alpha=0$ was used as input to deduce the Ga-Ga bond length. In this case, three different sets of phases and amplitudes were employed: (i) phases and amplitudes for the Ga-Te and Ga-Ga contributions from the FEFF code. As in the other orientation of the cell [method (ii) of the precedent paragraph], the resulting Ga-Ga bond length presented a considerable dispersion (Fig. 4, diamonds), (ii) phases and amplitudes for the Ga-Te backscattering process from the NaCl phase. It is worth noting that it is not possible to extract phases and amplitudes for the Ga-Ga backscattering process from the NaCl phase to study the low-pressure phase because of the high difference in the Ga-Ga distance between both phases. Thus we carried out the orientation-weighted difference between the spectra with $\alpha=90$ and $\alpha=0$ to extract the phases and amplitudes for the Ga-Ga backscattering process (Fig. 4, triangles), (iii) phases and amplitudes for the Ga-Te backscattering process from the NaCl phase and phases and amplitudes for the Ga-Ga backscattering process from the FEFF code. This last method presents the smallest dispersion in the resulting Ga-Ga bond length and is the more reliable method in our opinion (Fig. 4, squares). It also allows us to obtain the evolution under pressure of the Ga-Ga DW factor [Fig. 5(b)].

Due to the inferior quality of data for sample B with respect to sample A and the lack of spectra with the contributions from the Ga-Te and Ga-Ga backscattering processes

clearly detached, it was not possible to extend the analysis of the Ga-Ga bond length variation to sample B.

2. Structural changes

In the low-pressure phase, the pressure evolution of the Ga-Te and the in-plane Ga-Ga first neighbor distances have been fitted with a Murnaghan equation of state:

$$d = d_0\left(1+\frac{B_0}{B_0}P\right)^{-1/3B_0}, \tag{1}$$

where d_0 is the bond length distance at ambient conditions, B_0 is the isothermal bulk modulus at zero pressure, and B_0' its pressure derivative. For volume fits we substituted $3B_0'$ in the exponent by B_0'. The data dispersion prevents from obtaining B_0 and B_0' simultaneously. In order to obtain comparative values with other III-VI layered compounds, we have fixed, as in the case of GaSe (Ref. 27) and InSe,[26] B_0' to a value of 5. The fitting procedure yields the values

$$\text{Ga-Te:}\quad d_0 = 2.665\ \text{Å},\ B_0 = 124\pm 6\ \text{GPa},\ B_0' = 5, \tag{2a}$$

$$\text{in-plane Ga-Ga:}\quad d_0 = 2.436\ \text{Å},\ B_0 = 102\pm 8\ \text{GPa},\ B_0' = 5. \tag{2b}$$

The bulk modulus for the Ga-Te distance is very close to the ones obtained for Ga-Se in GaSe (Ref. 27) (90 ± 4 GPa) and In-Se in InSe (116 ± 20 GPa).[26]

The volume variation of the NaCl-type polymorph in the downstroke can also be fitted to a Murnaghan equation of state, giving $V_0 = 190\pm 5\ \text{Å}^3$, $B_0 = 58\pm 4$ GPa with B_0' fixed to 4.2. Our values are in perfect agreement with those obtained in Ref. 19 ($V_0 = 195\pm 1\ \text{Å}^3$, $B_0 = 60\pm 4$ GPa, and $B_0' = 4.2\pm 0.6$).

The variation of the Ga-Te distance with pressure is much slower than the variation found by x-ray studies for the c axis.[19] To make both values to be in agreement the angle between the Te planes and the Ga-Te bond (φ) must change. Because of the low symmetry of the unit cell, both φ and the intralayer Te-Te distance take different values. In average, the Te-Te distance in ambient conditions is $c_m = 4.33$ Å. With the aim of estimating the effect of pressure in φ, we calculate an average φ value through

$$\frac{c_m}{2} = d_{\text{GaTe}}\cos(\varphi)\cos 30°. \tag{2}$$

Equation (2) is exact in the other members of the III-VI layered family, where the cation-cation bond defines a symmetry axis of order 3. Next we suppose that c_m varies with pressure in the same way than the c axis does. With these considerations we can estimate that the average angle between the Ga-Te bond and the plane defined by the Te atoms increases with pressure at a rate of $0.23\pm 0.03°$/GPa, which represents a variation for φ from 20.2 ± 0.8 at ambient pressure to $22.6\pm 0.8°$ at the transition pressure. If we call ''base'' the face of the tetrahedron formed by the Te atoms, we can say that the ''base'' edge of the tetrahedron is decreasing under pressure more rapidly than its ''height.'' The small change of the in-plane Ga-Ga distance, as compared to the value of the compressibility along the direction perpendicular to the c axis ($\chi_{\perp c}$), also indicates an increase of the tilt angle of this bond with respect to the layer plane.

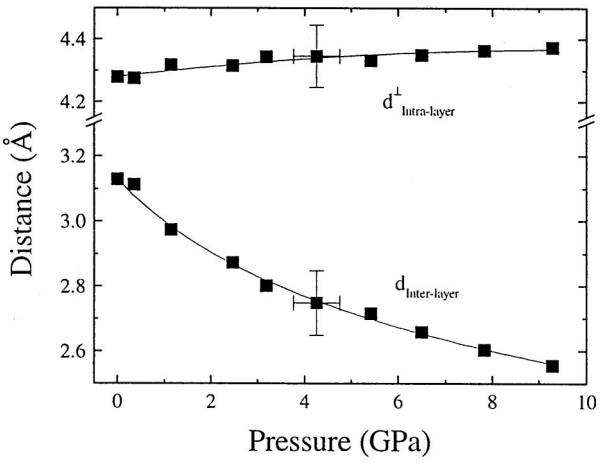

FIG. 6. Evolution under pressure of the intra- and interlayer distances in GaTe. The intralayer distance is the Te-Te distance measured in the direction perpendicular to the layers. The continuous lines are guides to the eye.

The structural changes inside the layer have implications on the evolution of intra- and interlayer distances. Following what happens in another simpler semiconductor of the same family, InSe,[26] we can estimate the evolution under pressure of the average inter- and intralayer distances as

$$d^{\perp}_{\text{intralayer}} = d^{\perp\,\text{layer}}_{\text{Ga-Ga}} + 2d_{\text{Ga-Te}}\sin\varphi, \tag{3a}$$

$$d_{\text{interlayer}} = d - d^{\perp}_{\text{intralayer}}, \tag{3b}$$

where d is thickness of the layer calculated from XRD data, $d_{\text{interlayer}}$ the interlayer distance, and $d^{\perp}_{\text{intralayer}}$ is the intralayer Te-Te distance in the direction perpendicular to the layers (opposed to c or c_m). Proceeding as in InSe, we assume that the bond length evolution under pressure is the same for the Ga-Te bond and for the Ga-Ga bond perpendicular to the layer plane, $d^{\perp\,\text{layer}}_{\text{Ga-Ga}}$. The inter- and intralayer distances (intralayer distance taken perpendicular to the layer) obtained in this way are presented in Fig. 6. Like in InSe, it is remarkable the slight increase of $d^{\perp}_{\text{intralayer}}$ with pressure. The augmentation is due to the fact that the increment of $2d_{\text{Ga-Te}}\sin(\varphi)$ is not compensated by the diminution in $d^{\perp\,\text{layer}}_{\text{Ga-Ga}}$. The evolution of the $d^{\perp}_{\text{intralayer}}$ distance in GaTe is similar to that of InSe, whereas the interlayer distance diminishes 6% less than in InSe. Although part of the difference could be absorbed by the experimental error both in the XRD and XAS data, the lower compressibility of the interlayer distance respect to InSe is understood as due to a higher interaction in the interlayer space caused by the tilt of the Te p_z orbitals and the bigger size of these orbitals with respect to the Se p_z ones.

The pressure evolution of the pseudo-Debye-Waller (DW) factors obtained in the EXAFS analysis is presented in Fig. 5. The DW factor gives an idea of the degree of both dynamic and static disorder. Combining the Einstein approximation with Raman-scattering data under pressure we can evaluate an approximation for the harmonic dynamic part of the DW (Refs. 37–39) factor. In InSe this calculation results in a diminution in the DW factor of the order of $10^{-4}\ \text{Å}^2$

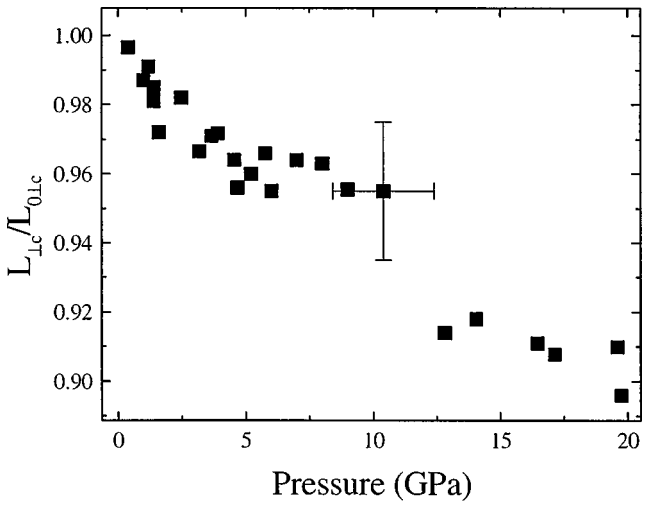

FIG. 7. Compressibility in the direction perpendicular to the *c* axis in the layer plane obtained by microphotographic measurements.

when pressure is increased from 0 to 10 GPa. For GaTe we can expect a variation of the same order of magnitude. Although the observed experimental decrease is slightly bigger, the small precision in the DW factor imposed by the normalization procedure of the spectra does not let us infer new conclusions. During the transition the DW factor increases because of the structural rearrangements. Along the downstroke process a structural destabilization is manifested through the increase of the static disorder. The loss of long-range translational order is evidenced by the even more important increase of static disorder corresponding to the second shell of neighbors [Fig. 5(b)].

C. Microphotographic measurements

The results of the photographic measurements are shown in Fig. 7. As commented in Sec. II, the compressibility along the *c* axis ($\chi_{\parallel c}$) is used as a gauge to determine the pressure. In the low-pressure phase we observe that $\chi_{\perp c}$ is nonlinear, decreasing as pressure approaches the transition value. As expected, in the NaCl high-pressure phase, within the experimental errors, $\chi_{\perp c}$ and $\chi_{\parallel c}$ become identical. The value found for the compressibility is compatible with the XRD experiment carried out in Ref. 19 for the low- and high-pressure phases.

The comparison of $\chi_{\parallel c}$ and $\chi_{\perp c}$ shows that distances in the direction perpendicular to the *c* axis shrink faster than those in the direction parallel to the *c* axis. As a result of the different compressibilities, the irregular hexagons formed by the Te atoms in the layer plane [Fig. 1(b)] tend to become more regular under pressure. This can be attributed to the fact that, when two layers approach, the strong interlayer repulsive forces tend to favor the close-packing sequence of Te atoms. The small change of the Ga-Ga distance, as compared to the value of $\chi_{\perp c}$, also indicates an increase of the tilt angle of this bond with respect to the layer plane. The $\chi_{\perp c}$ discontinuity in the transition is due to the filling of the volume in the region of the layer surrounding the Ga-Ga bonds parallel to the layer. With these considerations, it seems reasonable to attribute the main source of instability of the layer structure to the tilt of the Ga-Ga bond with respect to the layer plane.

IV. CONCLUSIONS

The evolution under pressure of the local structure in GaTe has been studied by XAS experiments at the Ga *K*-edge up to 14 GPa. The anisotropy of the sample is clearly manifested in the XAS spectra taken with different orientations of the sample respect to the synchrotron radiation polarization. The decomposition of the XANES part of the spectra into its low- and high-pressure components confirms the transition to a NaCl-type polymorph at 10.3 ± 1 GPa. The phase transition is nonreversible. In the downstroke a progressive amorphization of the sample is observed. The use of the polarization in the EXAFS analysis has let us determine both the Ga-Te and Ga-Ga bond lengths variations under pressure, in spite of the small amplitude of the latter. To quantify the evolution of the these bond lengths, a fit to a Murnaghan-type equation of state has been performed, resulting in an isothermal bulk modulus of 124 ± 6 and 102 ± 8 GPa for the Ga-Te and the in-plane Ga-Ga bond lengths, respectively (B_0' has been fixed to 5). As the GaTe low-pressure phase needs 18 structural parameters for a full description, our results are insufficient to carry out a detailed analysis of the evolution of the whole structure under pressure, as the one performed in InSe.[26] Nevertheless, combining our results with XRD ones,[19] we have estimated that in average the angle between the Ga-Te bond and the Te planes increases with pressure at a rate of $0.23 \pm 0.03°$/GPa. This increase is the final responsible of the augmentation found in the intralayer distance. The interlayer distances decrease in the same interval of pressures 6% less that in InSe due to the higher interlayer interaction in GaTe. In the high-pressure phase no difference between the local and bulk modulus has been found, obtaining an isothermal bulk modulus of 58 ± 4 GPa with B_0' fixed to 4.2. The study of the DW factors helps to follow the structural changes. In particular it informs us of the progressive amorphization of the sample in the downstroke, manifested through the increase of static disorder in the first two shells (Te and Ga) neighboring Ga atoms. The microphotographic measurements have let us compare the compressibility along the *c* axis with the compressibility in the direction perpendicular to the *c* axis in the layer plane, showing the tendency of the irregular atoms formed by the Te atoms to become regular under pressure, and bringing to evidence that the most important source of instability of the structure is the tilt with pressure of the Ga-Ga bonds that lay in the layer plane.

ACKNOWLEDGMENT

This work was supported by the Spanish government CICYT under Grant No. MAT95-0391.

*Author to whom correspondence should be addressed. FAX: (34) 96 3983146. Electronic address: Julio.Pellicer@uv.es

[1] A. Segura, J. P. Guesdon, J. M. Besson, and A. Chevy, J. Appl. Phys. **54**, 876 (1983).

[2] J. Martínez-Pastor, A. Segura, J. L. Valdés, and A. Chevy, J. Appl. Phys. **62**, 1477 (1987).
[3] O. Lang, R. Rudolph, A. Klein, C. Pettenkofer, W. Jaegermann, J. Sánchez, A. Segura, and A. Chevy, *Proceedings of the E. C. Photovoltaic Solar Energy Conference* (Reidel, Dordrecht, 1996), p. 2023.
[4] Ph. J. Kupecek, H. Le Person, and M. Comte, Infrared Phys. **19**, 263 (1979).
[5] C. Hirlimann, J. F. Morhange, M. A. Kanehisa, A. Chevy, and C. H. Brito Cruz, Appl. Phys. Lett. **55**, 2307 (1989).
[6] K. L. Vodopyanov, L. A. Kulevskii, V. G. Voevodin, A. I. Gribenyukov, K. R. Allakhverduev, and T. A. Kerimov, Opt. Commun. **83**, 322 (1991).
[7] E. Bringuier, A. Bourdon, N. Piccioli, and A. Chevy, Phys. Rev. B **49**, 16 971 (1994).
[8] M. A. Hernández, J. F. Sánchez, M. V. Andrés, A. Segura, and V. Muñoz, Óptica Pura y Aplicada **26**, 152 (1993).
[9] W. C. Eckhoff, R. S. Putnam, S. Wang, R. F. Curl, and F. K. Tittel, Appl. Phys. B: Lasers Opt. **63**, 437 (1996).
[10] V. K. Lukyanyuk, M. V. Tivarnitskii, and Z. D. Kovalyuk, Phys. Status Solidi A **104**, K41 (1987).
[11] M. Balkanski, C. Julien, and J. Y. Emery, J. Power Sources **26**, 615 (1989).
[12] E. Hatzikraniotis, C. Julien, and M. Balkanski, in *Solid State Batteries*, Vol. 101 of NATO *Advanced Study Institute; Series E: Applied Sciences*, edited by C. A. C. Squeira and A. Hooper (Martimes Nijhoff, Dordrecht, 1985), p. 479.
[13] *Semiconductors*, edited by O. Madelung, Landolt-Börnstein, New Series, Group III, Vol. 17, Pt. f (Springer-Verlag, Berlin, 1983).
[14] M. Julien-Pouzol, S. Jaulmes, M. Guittard, and F. Alapini, Acta Crystallogr., Sect. B: Struct. Crystallogr. Cryst. Chem. **B35**, 2848 (1979).
[15] J. F. Sánchez Royo, A. Segura, and V. Muñoz, Phys. Status Solidi A **151**, 257 (1995).
[16] A. Khun, A. Chevy, and R. Chevalier, Phys. Status Solidi A **31**, 469 (1975).
[17] J. Rigoult and A. Rimsky, Acta Crystallogr., Sect. B: Struct. Crystallogr. Cryst. Chem. **B36**, 916 (1980).
[18] A. J. Niilisk and J. J. Kirs, Phys. Status Solidi **31**, K97 (1969).
[19] U. Schwarz, K. Syassen, and R. Kniep, J. Alloys Compd. **224**, 212 (1995).
[20] J. Pellicer-Porres, F. J. Manjón, A. Segura, C. Power, J. Gonzalez, and V. Muñoz, Phys. Rev. B **60**, 8871 (1999).
[21] H. d'Amour, W. B. Holzapfel, A. Polian, and A. Chevy, Solid State Commun. **44**, 853 (1982).
[22] C. Ulrich, Ph.D. thesis, Max-Planck-Institut für Fesktkörperforschung, Stuttgart, 1997.
[23] D. C. Konigsberger and R. Prins, *X-ray Absorption: Principles, Applications, Techniques of EXAFS, SEXAFS and XANES* (Wiley Interscience, New York, 1988).
[24] J. P. Itié, V. Briois, D. Martinez, A. Polian, and A. San-Miguel, Phys. Status Solidi B **211**, 323 (1999).
[25] A. San Miguel, A. Polian, and J. P. Itié, Physica B **208&209**, 117 (1995).
[26] J. Pellicer-Porres, A. San Miguel, and V. Muñoz, Phys. Rev. B **60**, 3757 (1999).
[27] J. P. Itié, A. Polian, M. Gauthier, and A. San Miguel, in *Highlights ESRF 96-97*, edited by ESRF Information Office (ESRF, Grenoble, 1997), p. 58.
[28] J. C. Chervin, B. Canny, J. M. Besson, and Ph. Pruzan, Rev. Sci. Instrum. **66**, 2595 (1995).
[29] G. J. Piermarini and S. Block, Rev. Sci. Instrum. **46**, 973 (1975).
[30] M. Hagelstein, A. San Miguel, A. Fontaine, and J. Goulon, J. Phys. IV **7**, 303 (1997).
[31] J. Pellicer-Porres, A. San Miguel, and A. Fontaine, J. Synchrotron Radiat. **5**, 1250 (1998).
[32] H. Tolentino, F. Baudelet, E. Dartyge, A. Fontaine, A. Lena, and G. Tourillon, Nucl. Instrum. Methods Phys. Res. A **286**, 307 (1990).
[33] A. Polian, J. M. Besson, M. Grimsditch, and H. Vogt, Phys. Rev. B **25**, 2767 (1982).
[34] M. Gauthier, A. Polian, J. M. Besson, and A. Chevy, Phys. Rev. B **40**, 3837 (1989).
[35] J. P. Itié, A. Polian, G. Calas, J. Petiau, A. Fontaine, and H. Tolentino, Phys. Rev. Lett. **63**, 398 (1989).
[36] J. J. Rehr, S. I. Zabinsky, and R. C. Albers, Phys. Rev. Lett. **69**, 3397 (1992).
[37] G. Kress and J. Hafner, Phys. Rev. B **47**, 558 (1993).
[38] A. San Miguel, Ph.D. thesis, Université Paris VI, 1993.
[39] A. San Miguel, A. Polian, M. Gauthier, and J. P. Itié, Phys. Rev. B **48**, 8683 (1993).